Adiabatic B_1 Mapping for RF Current Density Imaging

K. Shultz[1], G. Scott[1], and J. Pauly[1]

[1]Electrical Engineering, Stanford University, Stanford, CA, United States

Introduction: RF current density imaging [1] can be used to predict RF ablation treatment patterns and to monitor the effectiveness of pacemaker insulators at RF frequencies. When the current is near the Larmor frequency, its associated magnetic field acts as a B_1 field, exciting magnetization. Due to the large variations and intensity of the local field and main field inhomogeneities near wires, typical B_1 measurement methods are impractical. We propose an adiabatic B_1 mapping pulse that covers a large dynamic range and compensates for B_0 variations.

Theory & Methods: Adiabatic excitation pulses are typically used because they create the same final flip angle for a wide range of B_1 magnitudes. However, if the end frequency of the pulse is not increased all the way to on-resonance, a B_1 magnitude dependent excitation results that can be used to map the B_1 field variation. The angle of the excitation and therefore the transverse magnetization is dependent on the B_1 strength, as shown in Figures 1 and 2. A large range of B_1 values can be distinguished from a single excitation.

A 90° adiabatic excitation is used as a reference to remove the dependence on the strength of the initial magnetization. The 90° excitation is also used to map the phase of B_1. Accurate phase mapping is particularly important for current density imaging.

Off-resonance acts as an additional frequency offset in the adiabatic pulse, changing the excitation frequency. For two different excitations with positive and negative excitation frequency offsets, the off-resonance will have the opposite effect on each and can be compensated.

The adiabatic pulse is a modified sech/tanh pulse, adapted using the method of Ugurbil et al [3] to cover a 16X dynamic range of B_1 and off-resonance of ±400 Hz. A typical ablation current of 1 A_{RMS} will create fields ranging from 0.14 to 1.4 G at distances between 1 mm and 1 cm from the wire. The pulse was optimized for this range, covering B_1 magnitudes from 0.1 to 1.6 G. Bloch simulations were performed for off-resonances from -400 to 400 Hz, T_1 of 500 ms, and T_2 of 50 ms with additive Gaussian noise. The double angle method for B_1 mapping [4] was also simulated for comparison with a 1.6 G pulse corresponding to a 90° rotation. A double angle sequence to fully cover the same range as the adiabatic pulse requires a series of 5 pulses from α to $2^4\alpha$ [5], two more than the adiabatic sequence.

To test the feasibility of using an adiabatic pulse to measure B_1 amplitude, experiments were run on a 1.5T GE Signa scanner with a phantom consisting of a wire with one inch exposed metal inserted into a tofu sample. Instead of using the 90° adiabatic excitation, the initial magnetization was assumed to be constant throughout the sample.

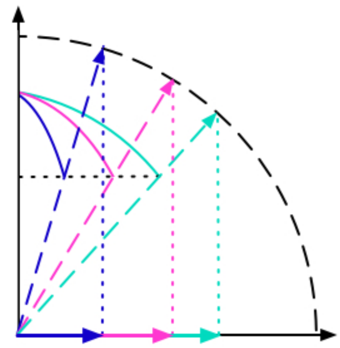

Figure 1: Sweep diagram [2] for adiabatic field mapping with various B_1 magnitudes. Each color represents a different B_1 magnitude. The solid arcs are the B_1 vector paths. The black dotted line represents the frequency where the excitation ends. The colored dashed lines are the magnetization vectors corresponding to the excitation angles. The solid colored arrows are the final transverse magnetization.

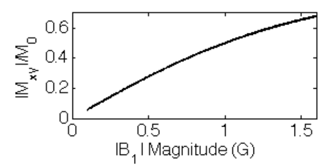

Figure 2: Transverse magnetization for adiabatic pulse with varying B_1 magnitude. The magnetization vs. magnitude is approximately linear over the 0.1 to 1.6 G range.

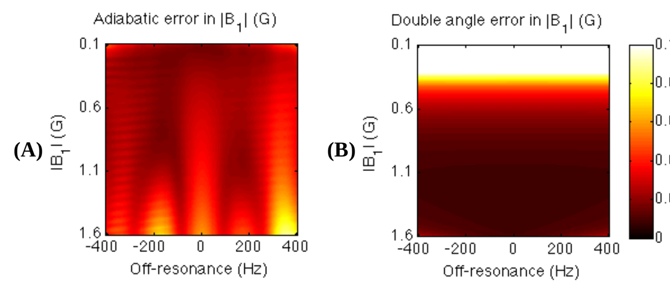

Figure 3: Simulated error in B_1 magnitude calculation (in Gauss) for the adiabatic method (A) and the double angle method (B). The adiabatic method covers a larger dynamic range without much loss in accuracy.

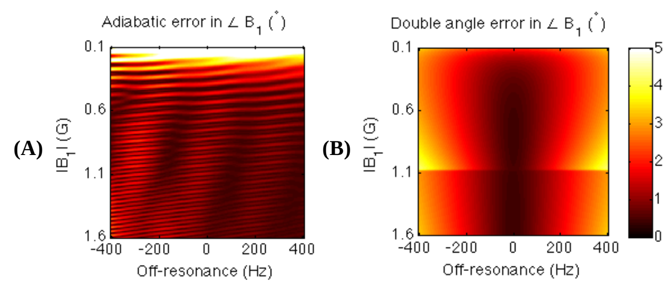

Figure 4: Simulated error in B_1 angle calculation (in degrees) for the adiabatic method (A) and the double angle method (B). The adiabatic method is more accurate except at low B_1 magnitudes.

Results: The root-mean-squared-error of the B_1 magnitude simulation results is shown in Figure 3. The double-angle pulse and the adiabatic pulse have similar accuracy for higher B_1 values, but the adiabatic pulse covers the entire dynamic range with similar accuracy. Figure 4 shows the simulated accuracy of the B_1 phase calculations. The performance of the adiabatic pulse suffers at low B_1 magnitudes, but it performs better than the double angle method for the rest of the range, particularly in areas with large off-resonance effects.

Figure 5 shows the reconstructed B_1 magnitude for a projection along the length of the wire in the phantom. There is signal dropout near the wire due to cancellation of the fields on opposite sides of the wire, as the projection axis is not perfectly aligned with the wire. The field drops off rapidly away from the wire, as expected.

Discussion & Conclusions: RF safety requires the ability to measure current levels and leakage from implanted wires. RF ablation treatment patterns can be predicted with the knowledge of current distributions. Current-carrying wires create large variations in B_1 magnitude near the wire while the presence of the wire creates inhomogeneity effects. The adiabatic B_1 mapping pulse can cover a 16X dynamic range in 60% of the time of a double angle sequence and has better performance in measuring the B_1 phase in the presence of off-resonance.

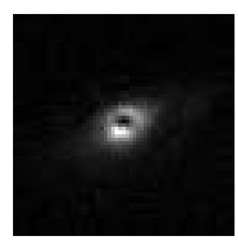

Figure 5: Reconstructed B_1 magnitude projection along length of wire in tofu phantom.

References: [1] G. Scott et al, Magn. Reson. Med. 28:186, 1992; [2] S. Conolly et al, J. Magn. Reson. 83:549, 1989; [3] K. Ugurbil et al, J. Magn. Reson. 80:448, 1988; [4] R. Stollberger et al, Proc 7th SMRM, p 106, 1988; [5] A. Kerr et al, Proc 15th ISMRM, p. 352, 2007